Journal of Soils and Sediments (2022) 22:682–691
https://doi.org/10.1007/s11368-022-03138-7

SEDIMENTS, SEC 2 • PHYSICAL AND BIOGEOCHEMICAL PROCESSES • RESEARCH ARTICLE

The anaerobic oxidation of methane driven by multiple electron acceptors suppresses the release of methane from the sediments of a reservoir

Xueping Chen[1] · Meilin Yang[1] · Jing Sun[1] · Juan Yu[1] · Lihua Liu[2] · Shuang Bai[1,3] · Fayan Bai[1] · Ming Yang[1] · Zheng Chen[4] · Chiquan He[1] · Xiaoyan Liu[1] · Jing Liang[5] · Fushun Wang[1]

Received: 2 October 2021 / Accepted: 9 January 2022 / Published online: 22 January 2022

Abstract

Purpose Methane, produced and emitted when organic carbon accumulates in reservoir sediments, can be oxidised microbially before being released into the overlying water by a variety of electron acceptors. This research aimed to investigate the microbial drivers responsible for the specific pattern of methane production and oxidation, as well as the role of electron acceptors in regulating anaerobic oxidation of methane (AOM) along the sediment core of a freshwater reservoir.

Materials and methods A sediment core was obtained from the Hongfeng Reservoir, a eutrophic lake-type reservoir located in Guizhou Province, China. To estimate methane production/oxidation profiles, the core was stratified and the porewater properties of each sediment layer (organic matter, carbon isotopic compositions, and etc.) were analysed and integrated with microbial communities and the methane production activity.

Results Methanogens were detected throughout the sediment depth profile. Hydrogenotrophic *Methanomicrobiales* were identified as the primary producer of methane in the surface layer (<20 cm), whereas *Methanobacteriales* and aceticlastic *Methanosarcinales* were revealed as the primary producers in the deeper layer. Additionally, methane was oxidised along the sediment profile with various electron acceptors. The coexistence of sulfate- and iron-oxidising bacteria at the surface layer demonstrated the possibility of sulfate and iron-dependent methane oxidation. Both the potential activity of AOM and the nitrite peak indicated the presence of an active nitrite-AOM zone consisted in the intermediate layer (14–24 cm) underneath the sulfate-AOM zone.

Conclusion Methane production and oxidation co-exist along the sediment core of a freshwater reservoir. Notably, AOMs have a significant potential to reduce in situ methane emissions from freshwater sediment environments. Additionally, there are multiple electrons available for the microbial AOM, and correspondingly, the functional microorganisms participating in AOMs are distributed across the sediment habitat in a niche-specific manner.

Keywords Methanogens · Methane oxidation · Methane emission · Microbial activity · Archaea

1 Introduction

There is growing interest and concern about greenhouse gas emissions from natural lakes and constructed reservoirs. These are one of the significant natural sources of methane, a greenhouse gas, with an estimated worldwide release of 12–70 Tg year^{-1} (Barros et al. 2011; Deemer et al. 2016), accounting for 6–16% of annual natural methane emissions (Goldman et al. 2016). Methane is produced in the anoxic sediments of lake/reservoir as a result of the microbial decomposition of organic matter. In addition, lake/reservoir sediments sequester a greater amount of extra labile organic materials than ocean sediments (Quadra et al. 2020). As a result, sediments in lakes/reservoirs are frequently regarded as 'hot spots' of methane production (Bastviken et al. 2004; He et al. 2018). While quantitative estimates of the terminal methane emission flux from lake/reservoir has been

Responsible editor: Haihan Zhang

✉ Lihua Liu
liulh@ms.giec.ac.cn

✉ Fushun Wang
fswang@shu.edu.cn

Extended author information available on the last page of the article

established through direct measurements and large-scale modelling (Maeck et al. 2013; Rosentreter et al. 2021), the transformation and mechanism of these events in sediments receive insufficient attention (Knittel and Boetius 2009).

Microbial activities regulate both the synthesis and consumption of methane in addition to methane diffusion and advection in sediments. It has been estimated that 50–95% (median of 90%) of the methane produced in freshwater lakes is oxidised prior to reaching the atmosphere (Bastviken et al. 2008). Methanotrophs oxidise methane biologically via aerobic and/or anaerobic processes. In lakes, the primary site of methane oxidation is expected to be in the oxic layer of sediments, or the layer of overlying water (Bastviken et al. 2008). However, recent study suggests that anaerobic oxidation of methane (AOM) (Wells et al. 2020) can occur in non-marine sediments via denitrification (Ettwig et al. 2010), sulfate reduction (Beal et al. 2009; Norði et al. 2013), and iron reduction via direct coupling or re-oxidation of sulfide (He et al. 2018).

Diverse biological niches for methane generation and consumption have been established in the complex sedimentary environment with multiple redox ions (Lloyd et al. 2011; Bodelier et al. 2013; Xiao et al. 2017; He et al. 2019). Denitrification, iron reduction, sulfate reduction, and methanogenic processes are listed in thermodynamic order based on the classical redox reaction sequence (Melton et al. 2014; Hansel et al. 2015). In the natural environment, however, certain reactions may overlap or reverse, and the boundaries of the reaction zone may even cross (Sela-Adler et al. 2017). Metal-AOM is found to exist directly below the oxic/anoxic boundary in iron-rich lake (Crowe et al. 2011) and below the zone of methanogenesis where nitrate and sulfate were entirely eliminated (Sivan et al. 2011). On the other hand, metal-AOM and sulfate-AOM were detected concurrently in the surface sediments of Lake Ørn (Norði and Thamdrup 2014). Additionally, anthropogenic eutrophication (Egger et al. 2015) and fast sediment deposition (Riedinger et al. 2014) could trigger the up-shift of sulphate-methane transition zone (SMTZ) in costal sediments. We hypothesise that, given the complex redox environment in reservoir sediments, methane production and oxidation may coexist in both freshwater as well as coastal sediments (Sivan et al. 2011; Xiao et al. 2017; Maltby et al. 2018), and that the geochemical gradient along a sediment profile may result in AOM niche differentiation depending on the electron acceptors.

We investigated a sediment core collected from Hongfeng Reservoir to explore the niche pattern of methane biological transformation. The reservoir is a lake-type reservoir with high concentration of nutrients and pollutants in its sediments, which have accumulated since the reservoir was constructed in 1958. In particular, we studied methane production and metabolism in freshwater sediments from the evidence of microbial colonisation combined with geochemical characteristics, focusing on the function of AOM driven by multi-electron acceptors on methane release from freshwater sediments. To achieve these objectives, the niche partitioning of methane production and oxidation were explored along the sediment core, through geochemical characteristics and microbial communities of samples in situ and lab incubation.

2 Materials and methods

2.1 Site description and sample collection

Hongfeng Reservoir is a eutrophic lake-type reservoir located in Qingzhen, Guizhou Province, China (106°19′–106°28′E, 26°26′–26°35′N; Fig. S1). The reservoir has a storage capacity of 6.01×10^8 m^3, and the average and maximum water depths are 10.5 m and 45 m, respectively. Surface water samples and one sediment core (diameter of 65 mm) were collected from the central area of the reservoir (106.4151° E, 26.478533° N) with a 10-m water depth in January 2017 (Fig. S1). The core was ~38 cm in length, and reached the soil layer corresponding to the period before the construction of the dam. The surface sediments (~1 cm) were dark brown (Fig. S1) and may have contained iron oxides, but the deeper sediments were black. The sediment core was sliced in situ into 1 cm (0–20 cm) or 2 cm (20–38 cm) sub-samples. Porewater was extracted simultaneously using a Rhizon sampler (Rhizosphere Research Products, The Netherlands) connected to vacuum sampling bottles, and was then stored at 4 °C. Some of the solid samples were frozen at −20 °C for DNA extraction and sequencing, and some were kept at 4 °C for later incubation. Aliquots of sediments were dried in an oven at 105 °C for 12 h and then filtered through a 200-mesh strainer. Some aliquots were powdered manually in an agate mortar for subsequent geochemical analysis.

2.2 Geochemical analytical methods

2.2.1 Sediment sample analyses

A subsample was decalcified with 10% HCl before being washed twice with deionised water and dried at 50 °C for the detection of total organic carbon (Donis et al. 2017) determination using a CHN-O rapid elemental analyser (Heaeus, Germany).

2.2.2 Determination of components and isotopic compositions of porewater

The concentrations of anions (SO_4^{2-} and NO_2^-) in the porewater were determined using an ion chromatographer (IC; ICS-1100, Thermo, CA, USA) equipped with a column of AG 19

(4 mm × 250 mm). The concentrations of formic acid, acetic acid, and propionic acid in porewater were analysed using an IC equipped with a column of Ion Pac AS11-HC (4 mm × 250 mm). Dissolved iron was determined by inductively coupled plasma mass-spectrometry (ICP–MS; Thermo iCAP Q, CA, USA) after samples were first diluted with 1% HNO_3.

The concentrations and stable carbon isotopic ($\delta^{13}C$) compositions of CH_4 and CO_2 from the porewater were determined by gas chromatography (GC; GC-C/TC III) isotoperatio mass spectrometry (IRMS; Delta V Advantage IRMS) and trace ultra GC (Thermo Finnigan). The chromatographic column was a HP-PLOT Q (30 m × 0.32 mm × 20.00 μm; J & W), and the injection temperature was 120 °C at a speed of 1.5 mL min^{-1}. The temperature of the burner was 960 °C, and that of the reducing furnace was 600 °C. The precision of the $\delta^{13}C_{CH4}$ and $\delta^{13}C_{CO2}$ measurements was ± 0.2‰. The concentration and carbon isotopic compositions of dissolved inorganic carbon (DIC) were determined using GasBench-IRMS (Delta V Advantage, USA).

2.3 Laboratory incubation

To measure the methane production potential, fresh sediment (equivalent to a 5.0 g dry weight) was placed into a 125 mL serum bottle using a cap-cut sterile syringe. The serum bottles with sediments were vacuumed and gas charged with N_2 for three cycles to achieve anaerobic conditions. The bottles were immediately sealed with thick butyl rubber stoppers and aluminium caps and incubated in a 25 °C incubator. In addition, sodium acetate (3.0 mmol kg^{-1}) was added as a substrate for methanogens. For the AOM potential measurement, the sediment incubation experiment was conducted as above, and was supplemented with methane at an initial concentration of approximately 8.3 mL L^{-1} after being sealed and N_2 replacement in the headspace. The headspace gas (1 mL) was collected by a micro-syringe for daily methane measurements. To maintain the ordinary pressure, 1 mL of pure N_2 was injected back into the bottle. The CH_4 concentration was determined by GC (GC-900, Shanghai Kechuang Chromatography Instrument Co. Shanghai, China) equipped with a hydrogen flame ionisation detector (FID), and expressed as per kilogram of dry weight (gdw) of sediment (Wassmann et al. 1998). All of the incubation experiments for methane production/oxidation potential were conducted in triplicate and, to the extent practicable, external contamination was avoided.

2.4 Microbial community

The DNA of sediment samples was extracted using a FastDNA® Spin Kit for Soil according to the manufacturer's instructions. The quality and concentration of the extracted DNA was assessed via spectroscopic analysis (NanoDrop Technologies).

2.4.1 Illumina sequencing and analysis

The microbial communities of the collected sediments were analysed by Illumina MiSeq sequencing. Microbial sequencing was performed using the MiSeq Illumina platform at Major Biotechnology Company (Shanghai, China) according to the methods of Caporaso et al. (2012). Briefly, the V3–V4 and V4 regions of 16S bacterial and archaeal ribosomal DNA (rDNA) were amplified, respectively. The custom degenerate primer pairs of barcode-338F (5′-ACTCCTACGGGAGGCAGC-3′)/907R (5′-CCGTCAATTC-MTTTRAGTTT-3′) (570 bp) and barcode-524F10extF (5′-TGYCAGCCGCCGCGGTAA-3′)/Arch958RmodR (5′-YCCGGCGTTGAVTCCAATT-3′) (434 bp) were used to generate an amplicon to construct libraries for bacteria and archaea, respectively. After sequencing, the quality of the raw data was checked (FastQC v0.11.8)) and filtered (PRINSEQ), and sequences less than 400 bp were eliminated from the resultant data. In total, 561,817 and 2,067,765 unique sequences were ultimately obtained for bacteria and archaea, respectively.

The sequence data were analysed using QIIME (version 1.17) (Deemer et al. 2016), and the sequences with a similarity of > 97% were clustered using Usearch (version 7.0, http://drive5.com/uparse/). This resulted in 6132 and 1885 operational taxonomic units (OTUs) for bacteria and archaea, respectively. The taxonomic assignment was performed using the Ribosomal Database Project (RDP) classifier (Goldman et al. 2016) and a training set extracted from the Silva108 database (Mendonça et al. 2012). Based on the results of the OTU clustering and annotation analysis, further data analysis was performed using the Mage's I-Sanger platform (http://www.i-sanger.com/), which integrates various R language packages for microbial community analysis. All sequences have been submitted to the Sequence Read Archive under the BioProject accession numbers SAMN09011655 to SAMN09011709.

2.4.2 Quantitative PCR

Copy numbers of the functional genes (*mcr*A) were determined by real-time polymerase chain reaction (PCR) using an iCycleriQ 5 thermocycler (Bio-Rad, CA, USA). The PCR primers were MLF (5′GGTGGTGTMGGATTCACACARTAYGCWACAGC3′) and MLR (TTCATTGCRTAGTTWGGRTAGTT). To optimise the real-time PCR reaction system, some DNA extracts were diluted 100-fold or tenfold and used as a template. Serial plasmid dilutions of

the respective functional genes (2.3×10^3 to 2.3×10^8 per action, $r^2=0.99$) were employed as standards. All of the template DNA and standard samples were conducted in triplicate. The 20 µL reaction mixtures included 1 µL of template DNA, 12.0 µL of SYBR Premix Ex Taq (Takara BioInc, Shiga, Japan), and 500 nM of each primer. All PCR runs began with an initial denaturation at 95 °C for 5 min, 94 °C for 1 min, 55 °C for 1 min, and 72 °C for 30 s. This was followed by a melting curve analysis from 65 to 98 °C at 0.2 °C per reading with a 6-s hold time. Fluorescence was read during each cycle at 83 °C.

3 Results

3.1 Carbon content and carbon isotopic signature

The $\delta^{13}C_{CH4}$ value (Vienna Pee Dee Belemnite, VPDB) decreased from −50.0‰ at the sediment surface to less than −68.1‰ at a depth of 11 cm, and then remained relatively constant between −68.1 and −70.2‰ below 12 cm (Fig. 1A). The values of $\delta^{13}C_{CO2}$ (VPDB) and $\delta^{13}C_{DIC}$ (VPDB) varied proportionally and inversely with respect to the $\delta^{13}C_{CH4}$ values. The $\delta^{13}C_{CO2}$ and $\delta^{13}C_{DIC}$ values were nearly constant for the first 3 cm (−16‰ and −8‰, respectively), and subsequently increased below a depth of 12 cm to relatively constant values of between −1.15 and −2.68‰ for $\delta^{13}C_{CO2}$, and between 2.70 and 6.40‰ for $\delta^{13}C_{DIC}$.

The TOC content (Fig. 1E) fluctuated between from 1.3 and 4 wt%, with a peak of 3.5–4.0 wt% at a depth of 10–17 cm. The TOC content decreased with two steps above and below the peak. The TOC content in the 3–8 cm layer was comparable to that in the 19–22 cm layer (2.2–2.3 wt%). The TOC content in the first 2 cm and 23–24 cm layer was 1.9 wt% and 2.2 wt%, respectively, and was relatively constant down the core at ~1.5 wt%.

The concentration profiles of methane, nitrate, iron, and sulfate are shown in Fig. 1B–E. The methane concentration increased from the top surface (0.054 mM) to the 10–11 cm layer (1.5 mM), and then declined quickly to 0.040 mM at a depth of 13 cm, it subsequently increased to 0.94 mM at a depth of 17 cm, and fluctuated between 0.025 and 0.58 mM below 18 cm (Fig. 1B). The nitrite concentration decreased from 10 µM at the surface to 5 µM at a depth of 5 cm, and then increased to 40 µM at a depth of 14 cm. It subsequently reduced to 16–23 µM at a depth of 16–24 cm before remaining relatively constant down the remaining core (Fig. 1B). The sulfate concentration decreased from 0.6 mM at the surface to less than 0.1 mM at 10–12 cm, which was followed by a high value at ~13 cm and then relatively constant values of 0.04–0.1 mM down the remaining core (Fig. 1C). The iron concentration declined from 44 µM at the surface to 24 µM at a depth of 4 cm, and was then relatively constant at ~10 µM down the rest of the core (Fig. 1D).

3.2 Incubation results for methanogens and anaerobic methanotrophs

The incubation results for the methane production potential both without and with methanogenic substrate (i.e. sodium acetate), and the consumption potential are shown in Fig. 2A–C. The methane production rate was comparatively high (0.03–3.94 µg CH_4 g^{-1} sediment d^{-1}) in sediments at a depth of 0–13 cm, and decreased along the core with the exception of that at ~20 cm (0.19 µg CH_4 g^{-1} sediment d^{-1}) (Fig. 2A). Moreover, the methane production rate increased dramatically in the treatment that included sodium acetate, especially at a depth of > 10 cm (Fig. 2B).

Because all of the sediments showed a high potential of AOM during the first 2 months of incubation, the following discussion based on this period (Fig. 2C). An extraordinarily high value (6.47 µg CH_4 g^{-1} sediment d^{-1}) was measured at a depth of ~18 cm, followed by a fast decline. Another active AOM zone was observed at a depth of 5–10 cm (1.37–2.14 µg CH_4 g^{-1} sediment d^{-1}).

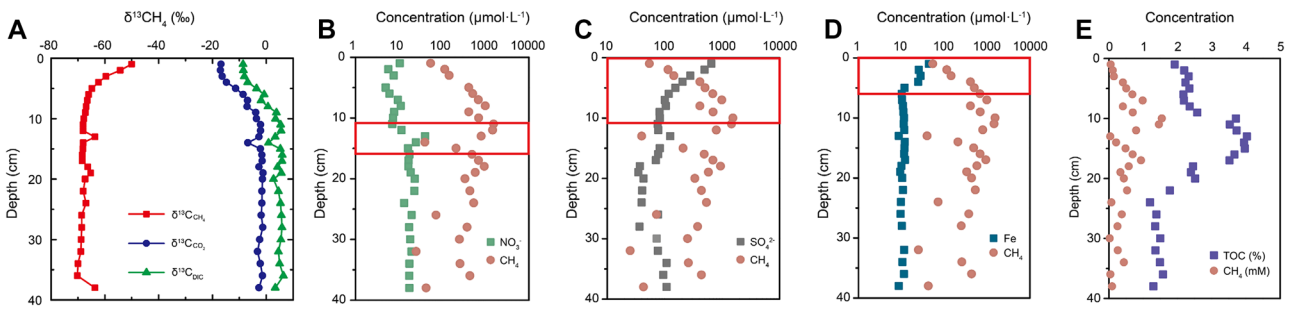

Fig. 1 Profiles of methane and carbon isotopic compositions of methane, CO_2, and DIC (VPDB) (**A**), nitrite (**B**), sulfate (**C**), iron (**D**), and TOC (**E**) in the sediment porewater in the Hongfeng Reservoir. DIC and TOC stand for dissolved inorganic carbon and total organic carbon. The squares in **B**, **C**, and **D** outline the inferred AOM zones discussed in the zonation of AOM

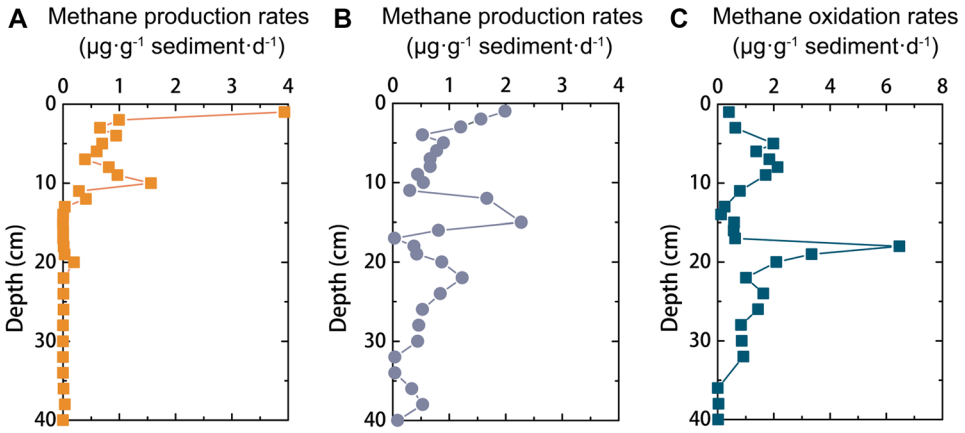

Fig. 2 The methane production rates along the sediment profile incubated without substrate (**A**) and with acetate (**B**), and the anaerobic methane oxidation rates along the sediment profile (**C**) in the Hongfeng Reservoir

3.3 Potential methanogen species and functional species involved in AOM

Functional molecular genetic markers that are specific to methanogens were quantified by real-time qPCR (Fig. 3A). The *mcr*A gene copy numbers were relatively constant throughout the core, although there were two peaks at 12 cm (6.72×10^7 copies g^{-1} sediment) and 22 cm (4.92×10^7 copies g^{-1} sediment).

The archaea community in the sediments was dominated by *Euryarchaeota* and *Bathyarchaeota*, which collectively accounted for 76.0–85.1% of the total community (Fig. S2B). The main methanogens in the sediments were *Methanosarcinales* (3.09–29.18%), *Methanomicrobiales* (0.55–14.23%), and *Methanobacteriales* (0.69–8.23%) at the order level (Fig. 3B; Fig. S2). Interestingly, *Methanobacteriales* was mainly distributed at a depth of 6–18 cm (1.17–8.23%), whereas its relative abundance in the surface layer (1–5 cm) was < 0.78% and disappeared below 18 cm (< 0.01%). The abundance of *Methanomicrobiales* in the sediments was slightly higher above a depth of 15 cm (3.86–14.23%) than of that below 16 cm (0.55–4.79%).

The Illumina sequencing results showed diverse and abundant functional groups involved in NO_3^-/NO_2^-, SO_4^{2-}, and metal-dependent anaerobic methane oxidation (Fig. 4; Fig. S3). The abundance of typical nitrite-dependent anaerobic methane oxidation bacteria (*Candidatus Methylomirabilis oxyfera*) was significantly higher below 18 cm (40.2–48.7%) than at shallower depths (0–17 cm, 31.7–38.2%) (Fig. 4B). Nitrate-dependent AOM was performed by ANME-2d, and which was mostly prevalent in the upper layers (0–19 cm, 1.6–6.5%), and that the relative abundance varied in a narrow range of 0.60–0.98% below a depth of 20 cm (Fig. 4B). The abundance of ANME-2d in the sediments was higher above a depth of 18 cm (0.640–2.23%) in comparison to below 18 cm (0.23%; Fig. 4B). For the archaeal anaerobic methanotrophs in the sediment, the groups of ANME-1a/b, ANME-3 were observed along the sediment profile (Fig. 4A). The relative abundance of ANME-1a/b

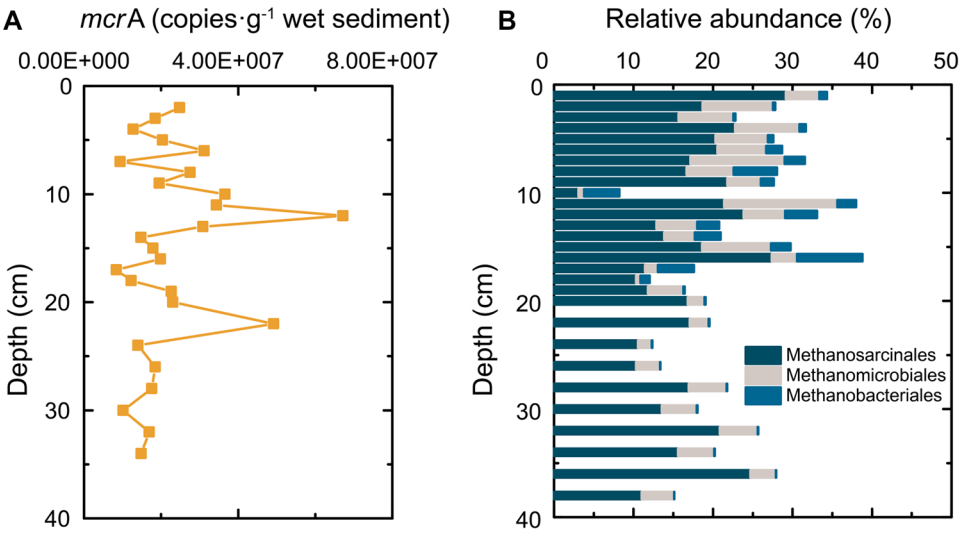

Fig. 3 The abundance of *mcr*A gene (**A**) and the relative abundance (**B**) of dominate methanogens at order level detected along the sediment profile in the Hongfeng Reservoir

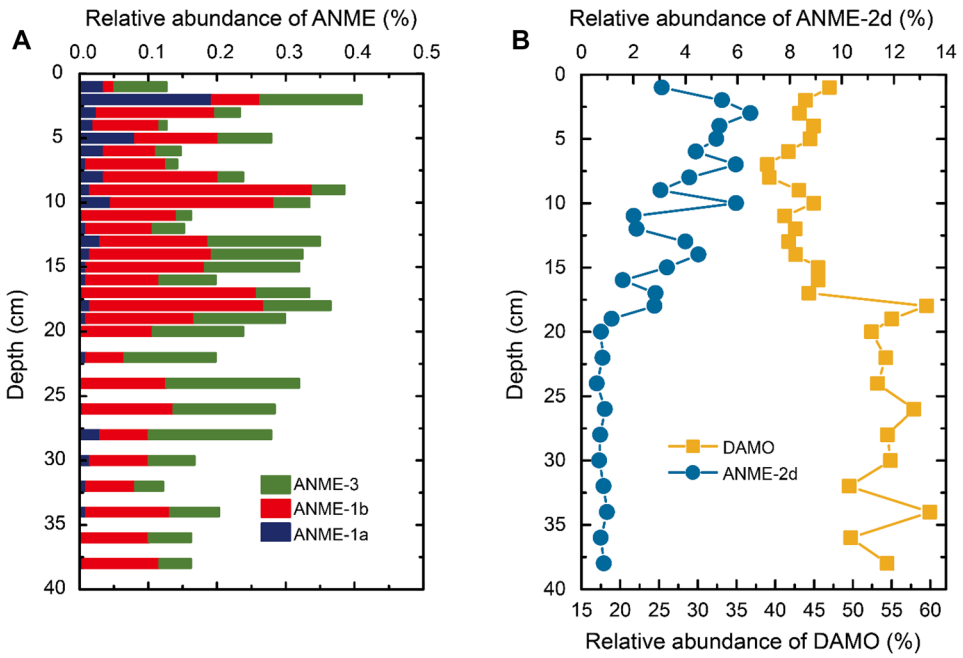

Fig. 4 The relative abundance of *ANMEs* (**A**), *M.oxyfera* and ANME-2d (**B**) along the sediment profile in the Hongfeng Reservoir

was higher than ANME-3 above a depth of 18 cm, but this tendency was totally reversed below the depth of 20 cm. The relative abundance of ANME-1a varied in a narrow range of 0–0.081%, with the exception of a high value of 0.193% at 2 cm (Fig. 4A). The ANME-1b was increased with the depth in the surface layers (0–3 cm), and peaked at 9–18 cm (0.096–0.324%). The abundance of ANME-3 was similarly increased in the upper 3 cm (up to 0.147%) in the sediments, which was higher in the depth of 13–28 cm (0.076–0.162%) in comparison to other layers (< 0.06%; Fig. 4A).

4 Discussion

4.1 Intersecting of methane production and consumption

The opposite trends of the porewater profiles of the $\delta^{13}C_{CH4}$ value versus the $\delta^{13}C_{CO2}$ and $\delta^{13}C_{DIC}$ (Fig. 1A) indicated a typical methane cycle zonation, with a clear zone of methane oxidation dominated the upper sediments (< 10 cm), and methane production prevailed in the lower sediments (> 10 cm). When plotted against the logarithmic methane concentrations (Fig. S4), and after eliminating the residual heavy methane, a linear trend of the $\delta^{13}C_{CH4}$ value suggests that methane was oxidised in the sediments, whereby the corresponding $\delta^{13}C_{DIC}$ were more positive (−8.6 to > 3‰ VPDB). The aerobic consumption of methane obviously occurred in the very top surface (< 1 cm) (Fig. S1) because oxygen can penetrate (< 8 mm) to this depth, even in an oligotrophic lake (Melton et al. 2014). The sediments became anaerobic while oxygen decreased rapidly with increasing sediment depth, which led to a shift in methane consumption to anaerobic oxidation. As Lloyd et al. (2011), Norði et al. (2013), and Riedinger et al. (2014) reported, the symmetrical concentration profiles of methane versus sulfate, iron, and nitrate/nitrite (Fig. 1B–D) suggest that methane oxidation may have been coupled with sulfate (< 10 cm), iron (< 5 cm) and nitrite separately (12–24 cm). There may be the impact of organic matter (humic substance) especially on the surface sediment, but we were unable to completely rule out it in this study.

The lab incubation data demonstrated the high potential of both anaerobic methane production and oxidation along the entire depth of the sediment core (Fig. 5) (Heuer et al. 2010; Norði et al. 2013; Norði and Thamdrup 2014; Mach et al. 2015; Rissanen et al. 2021a, b; Yang et al. 2021). Interestingly, the methane production rate was obviously higher at a depth of 0–13 cm than that at ≥ 14 cm (Fig. 2A), and only when the extra substrate was added did the production rates increase dramatically (> 10 cm) to exceed those in the surface sediment (Fig. 2B). In accordance with the geochemical data, an extremely high activity of methane oxidation was identified at ~18 cm (Fig. 2C). Another active AOM zone was observed at 5–10 cm, which agreed with the changes in the electron acceptors (Fig. 1B−D). Therefore, methane production and consumption multiplied along the sediment core, and the consumption potential was much higher than production with or without additional substrate (Su et al. 2019).

To sum up, the coexistence methane production and oxidation was proven by the two distinct production zones that

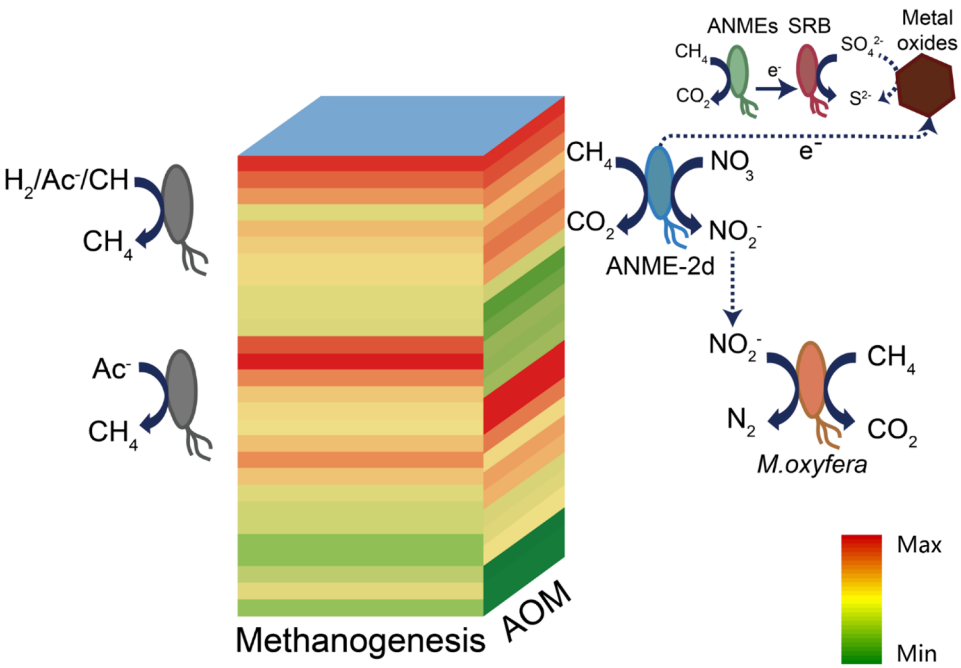

Fig. 5 Schematic representation of methane production and oxidation along the sediment core profile in the Hongfeng Reservoir. The relative microbial activity of functional groups, involved in the methanogenesis and methanotrophs, is indicated by color. The AOM process is driven by anaerobic methane oxidising bacteria (ANME), sulfate reducing bacteria (SRB), and *M. oxyfera*

were parallel to two evident AOM zones (Figs. 2 and 5), rather than the stereotypical pattern of oxidation/production along the redox gradient.

4.2 Zonation of methane production and limitation

4.2.1 Abundant methanogens along the sediments core

Abundance functional gene of methanogenic (methyl-coenzyme M reductase, *mcr*A gene) existed along the sediment core profile (Fig. 3A). Within the top 10 cm, higher abundance of the *mcr*A gene corresponded to the more vigorous potential of methane production.

The copy numbers of the *mcr*A gene (Fig. 3A) matched the methane production potential with substrate addition (Fig. 2B), which indicated that methanogens were stimulated by sufficient substrate and became active. This pattern was obvious at a depth of 10–17 cm, where the high TOC content and the anaerobic environment facilitated anaerobic digestion. The metabolic production might have also furthered promoted the growth of methanogens (e.g. via a hydrogenotrophic pathway) (Chen et al. 2021). Therefore, the activity of methanogenesis was constrained by the bioavailable substrate rather than by the abundance of methanogens.

4.2.2 Niche partitioning of various nutrient types of methanogens along the sediment core

The vertical distribution of various nutrient types of methanogens was revealed along the sediment core profile (Fig. 3B). Correspondingly, *Methanomicrobiales* and *Methanobacteriales* were mainly distributed within the upper ~20 cm. These hydrogenotrophic methanogens are able to produce methane using compounds containing H_2, CO_2, formic acid, alcohol, and propanol as energy and carbon sources (Euler et al. 2020). Therefore, hydrogenotrophic might have been an active methanogenic pathway in the upper layers. The relative abundance of *Methanobacteriales* peaked at 10–17 cm, and then disappeared below 18 cm (< 0.01%), which demonstrates the critical role of *Methanobacteriales* in such a fermentation layer.

The dominant methanogens were *Methanosarcinales*, which mainly consist of *Methanothrix* at the genus level, and are typical aceticlastic methanogens. When supplemented with sodium acetate, *Methanothrix* recovered the activity of methane production in the deeper layers. *Methanothrix* is an obligate aceticlastic methanogenic archaeon that can adapt to low concentrations of acetic acid of 7–70 μmol L^{-1} (Westermann et al. 1989) due to acetyl-CoA synthetase with a high affinity to acetic acid (Jetten et al. 1990). In general, there is a large amount of nutrients and organic matter sequestrated in the sediments of reservoirs (e.g. sodium acetate) (Quadra et al. 2020). Hence, aceticlastic methanogens dominate and play a critical role in methane production in deep sediments (Scholten and Stams 2000).

4.3 Zonation of methane oxidation and metabolism

A complex oxidation pattern was discovered in the sediment cores. With the exception of the top surface layer (< 1 cm) that may have been oxidised by oxygen, methane consumption in the deeper layers was coupled with SO_4^{2-}-AOM,

metal-AOM, and NO_3^-/NO_2^--AOM (Figs. 1, 2, and 4; Fig. S3). Mayr et al. (2020) recently found such a niche partitioning of the taxa of different methane oxidisers in four lake sediments, which effectively mediated methane oxidation along with the oxygen–methane counter gradient. The functional groups involved in these processes include the consortia of anaerobic methanotrophic archaea, particular sulfate reducing bacteria (*Desulfobulbus*) (Bhattarai et al. 2019), ferric iron reducing bacteria (*Geobacter*) (Gao et al. 2017) and NC10 (Lee et al. 2018).

4.3.1 SO_4^{2}–AOM and metal–AOM in the subsurface layer

The profiles of oxidants and functional groups indicate that sulfate was the primary oxidant for AOM in the surface layer (< 10 cm) and at ~13 cm, and subsequently drove the apparent iron oxides to mediate AOM (< 5 cm), which is similar to the report of He et al. (2018). The relative abundance of ANME and *Desulfobulbus* in the upper layer confirmed the interdependence of sulfate reducing bacteria and AOM. The reduced sulfur may have then transferred electrons to iron oxides, which could have been further driven by microbial iron oxidation performed by the identified iron-oxidising bacteria of *Ferritrophicum* and *Crenothrix* (0–17 cm). The relative high abundance of ANME-2d was demonstrated to potentially transfer the elements by extracellular electron transfer (Oni and Friedrich 2017) and interspecific electron transfer (Cai et al. 2018). Melton et al. (2014) demonstrated that Fe oxidisers could overcome the competition pressure to survive in lake sediments resulting in a high abundance of poorly crystalline iron. Norði et al. (2013) observed that ANME-2d drived AOM in iron-rich freshwater lake sediments where sulfate and Fe(III) coexisted. Unfortunately, although Cai et al. (2018) reported the enrichment and characterisation of a novel archaeon *Candidatus* "*Methanoperedens ferrireducens*" which couples anaerobic oxidation of methane to Fe(III) reduction, the responsible microorganisms for metal-AOM are still difficult to define. The potential of iron-AOM is uncertain in our study due to the preferential sulfate reduction and undetected iron minerals.

4.3.2 denitrification–AOM in the middle layer

Both of the incubation activity (Fig. 2C) and carbon isotope composition (Fig. 1A) of the sediments indicated the presence of an AOM zone in the intermediate layer of the sediments (18–20 cm). Correspondingly, abundant of nitrate- (*Can. Methanoperedens* and ANME-2d) and nitrite-dependent (NC10, *M. oxyfera*) methane anaerobic-oxidation microorganisms (Kurth et al. 2019) were concurrence at the depth of 18–20 cm. In a strictly anoxic environment, the coexistence of CH_4, NO_2^-/NO_3^- drove the AOM (Lee et al. 2018). ANME-2d archaea can independently complete the nitrate-driven anaerobic oxidation reaction of methane without the participation of other microorganisms, which can reduce nitrate to nitrite while oxidising methane (Haroon et al. 2013). Furthermore, ANME-2d archaea has been found in many reactors to be coexist with *M. oxyfera* bacteria (Hu et al. 2015; Lomakina et al. 2019). Recently, Nie et al. (2021) found that ANME-2d is syntrophic with NC10 via microbial metabolites exchange within consortia for simultaneous nitrate- and sulfate-dependent AOM. In collaboration with sulfate-reducing bacteria (SRB) and iron reducing bacteria, active ANME-2d would provide a connection between the carbon, nitrogen, iron and sulfur cycles occurring in freshwater environments. Therefore, the anaerobic zone of freshwater sediments is an ideal habitat for the N-DAMO reaction as reported in lake ecosystems (Deutzmann and Schink 2011; Mayr et al. 2020).

5 Conclusion

An interaction intersecting zonation of methane production and oxidation has been revealed in the freshwater sediments based on the porewater concentration of methane, carbon isotopic composition, the incubation activity, and the abundance of functional genes. That is, two distinct AOM zones were concurrent with two production zones. The availability of substrate controls the production ability more than abundance and diversity of methanogens, simultaneously, and the abundance and activity of functional microorganisms of AOM are critical for quantifying the aquatic methane efflux from such environments. This study sheds new light on the metabolism and mechanism behind the biogeochemical cycles for carbon, sulfur, nitrogen, and metals in reservoir sediments. Furthermore, the critical role of AOM in mitigating methane release from the reservoir has been confirmed, which can help to better remedy the widespread methane emissions from freshwater sediments.

Supplementary Information The online version contains supplementary material available at https://doi.org/10.1007/s11368-022-03138-7.

Author contribution F. Wang conceived and supervised the study. L. Liu, X. Chen designed the experiments. X. Chen, J. Yu, F. Bai, M. Yang, S. Bai, and Z. Chen performed the experiments. X. Chen, F. Bai, S. Bai, C. He, X. Liu, and J. Liang analysed the data. X. Chen, L. Liu, Z. Chen, J. Yu, and J. Sun wrote the manuscript. J. Liang revised the language express of manuscript.

Funding This work was supported by the National Key Research and Development Project by Most of China (grant number 2016YFA0601000), National Natural Science Foundation of China (grant numbers 41776071, 41073072, 21677093), the Shanghai Science and Technology Committee (grant number 12231202004), Guangdong MEPP Fund (NO. GDOE[2019]A41), and Natural Science Foundation of Shanghai (21DZ1209403).

Declarations

Competing interests The authors declare no competing interests.

References

Barros N, Cole JJ, Tranvik LJ, Prairie YT, Bastviken D, Huszar VLM, del Giorgio P, Roland F (2011) Carbon emission from hydroelectric reservoirs linked to reservoir age and latitude. Nat Geosci 4:593–596

Bastviken D, Cole J, Pace M, Tranvik L (2004) Methane emissions from lakes: dependence of lake characteristics, two regional assessments, and a global estimate. Global Biogeochem Cy 18:1–12

Bastviken D, Cole JJ, Pace ML, Van de Bogert MC (2008) Fates of methane from different lake habitats: connecting whole-lake budgets and ch4emissions. J Geophys Res: Biogeosci 113:1–13

Beal EJ, House CH, Orphan VJ (2009) Manganese- and iron-dependent marine methane oxidation. Science 325:184–187

Bhattarai S, Cassarini C, Lens PNL (2019) Physiology and distribution of archaeal methanotrophs that couple anaerobic oxidation of methane with sulfate reduction. Microbiol Mol Biol R 83:1–31

Bodelier PL, Meima-Franke M, Hordijk CA, Steenbergh AK, Hefting MM, Bodrossy L, von Bergen M, Seifert J (2013) Microbial minorities modulate methane consumption through niche partitioning. ISME J 7:2214–2228

Cai C, Leu AO, Xie GJ, Guo J, Feng Y, Zhao JX, Tyson GW, Yuan Z, Hu S (2018) A methanotrophic archaeon couples anaerobic oxidation of methane to Fe(III) reduction. ISME J 12:1929–1939

Caporaso JG, Lauber CL, Walters WA, Berg-Lyons D, Huntley J, Fierer N, Owens SM, Betley J, Fraser L, Bauer M, Gormley N, Gilbert JA, Smith G, Knight R (2012) Ultra-high-throughput microbial community analysis on the Illumina Hiseq and Miseq platforms. ISME J 6:1621–1624

Chen H, Wang Z, Liu H, Nie Y, Zhu Y, Jia Q, Ding G, Ye J (2021) Variable sediment methane production in response to different source-associated sewer sediment types and hydrological patterns: Role of the sediment microbiome. Water Res 190:116670

Crowe SA, Katsev S, Leslie K, Sturm A, Magen C, Nomosatryo S, Pack MA, Kessler JD, Reeburgh WS, Roberts JA, Gonzalez L, Douglas Haffner G, Mucci A, Sundby B, Fowle DA (2011) The methane cycle in ferruginous lake matano. Geobiol 9:61–78

Deemer BR, Harrison JA, Li S, Beaulieu JJ, DelSontro T, Barros N, Bezerra-Neto JF, Powers SM, Dos Santos MA, Vonk JA (2016) Greenhouse gas emissions from reservoir water surfaces: a new global synthesis. Bioscience 66:949–964

Deutzmann JS, Schink B (2011) Anaerobic oxidation of methane in sediments of lake constance, an oligotrophic freshwater lake. Appl Environ Microb 77:4429–4436

Donis D, Flury S, Stockli A, Spangenberg JE, Vachon D, McGinnis DF (2017) Full-scale evaluation of methane production under oxic conditions in a mesotrophic lake. Nat Commun 8:1661

Egger M, Rasigraf O, Sapart CJ, Jilbert T, Jetten MS, Rockmann T, van der Veen C, Banda N, Kartal B, Ettwig KF, Slomp CP (2015) Iron-mediated anaerobic oxidation of methane in brackish coastal sediments. Environ Sci Technol 49:277–283

Ettwig KF et al (2010) Nitrite-driven anaerobic methane oxidation by oxygenic bacteria. Nature 464:543–548

Euler S, Jeffrey LC, Maher DT, Mackenzie D, Tait DR (2020) Shifts in methanogenic archaea communities and methane dynamics along a subtropical estuarine land use gradient. PLoS One 15:e0242339

Gao Y, Lee J, Neufeld JD, Park J, Rittmann BE, Lee HS (2017) Anaerobic oxidation of methane coupled with extracellular electron transfer to electrodes. Sci Rep 7:5099

Goldman AE, Cadieux SB, White JR, Pratt LM (2016) Passive sampling method for high-resolution concentration and isotopic composition of dissolved methane in arctic lakes. Limnol Oceanogr-Methods 14:69–78

Hansel CM, Lentini CJ, Tang Y, Johnston DT, Wankel SD, Jardine PM (2015) Dominance of sulfur-fueled iron oxide reduction in low-sulfate freshwater sediments. ISME J 9:2400–2412

Haroon MF, Hu S, Shi Y, Imelfort M, Keller J, Hugenholtz P, Yuan Z, Tyson GW (2013) Anaerobic oxidation of methane coupled to nitrate reduction in a novel archaeal lineage. Nature 500:567–570

He Q, Yu L, Li J, He D, Cai X, Zhou S (2019) Electron shuttles enhance anaerobic oxidation of methane coupled to iron(iii) reduction. Sci Total Environ 688:664–672

He Z, Zhang Q, Feng Y, Luo H, Pan X, Gadd GM (2018) Microbiological and environmental significance of metal-dependent anaerobic oxidation of methane. Sci Total Environ 610–611:759–768

Heuer VB, Krüger M, Elvert M, Hinrichs K-U (2010) Experimental studies on the stable carbon isotope biogeochemistry of acetate in lake sediments. Org Geochem 41:22–30

Hu S, Zeng RJ, Haroon MF, Keller J, Lant PA, Tyson GW, Yuan Z (2015) A laboratory investigation of interactions between denitrifying anaerobic methane oxidation (DAMO) and anammox processes in anoxic environments. Sci Rep 5:8706

Jetten MSM, Stams AJM, Zehnder AJB (1990) Acetate threshold values and acetate activating enzymes in methanogenic bacteria. FEMS Microbiol Ecol 73:339–344

Knittel K, Boetius A (2009) Anaerobic oxidation of methane: progress with an unknown process. Annu Rev Microbiol 63:311–334

Kurth JM, Smit NT, Berger S, Schouten S, Jetten MSM, Welte CU (2019) Anaerobic methanotrophic archaea of the ANME-2d clade feature lipid composition that differs from other ANME archaea. FEMS Microbiol Ecol 95:fiz082

Lee HS, Tang Y, Rittmann BE, Zhao HP (2018) Anaerobic oxidation of methane coupled to denitrification: fundamentals, challenges, and potential. Crit Rev Envi Sci Tec 48:1067–1093

Lloyd KG, Alperin MJ, Teske A (2011) Environmental evidence for net methane production and oxidation in putative anaerobic methanotrophic (ANME) archaea. Environ Microbiol 13:2548–2564

Lomakina A, Pogodaeva T, Kalmychkov G, Chernitsyna S, Zemskaya T (2019) Diversity of NC10 bacteria and ANME-2d archaea in sediments of fault zones at Lake Baikal. Diversity 12:10

Mach V, Blaser MB, Claus P, Chaudhary PP, Rulik M (2015) Methane production potentials, pathways, and communities of methanogens in vertical sediment profiles of river sitka. Front Microbiol 6:506

Maeck A, Delsontro T, McGinnis DF, Fischer H, Flury S, Schmidt M, Fietzek P, Lorke A (2013) Sediment trapping by dams creates methane emission hot spots. Environ Sci Technol 47:8130–8137

Maltby J, Steinle L, Löscher CR, Bange HW, Fischer MA, Schmidt M, Treude T (2018) Microbial methanogenesis in the sulfate-reducing zone of sediments in the EckernfördeBay, sw Baltic Sea. Biogeosciences 15:137–157

Mayr MJ, Zimmermann M, Guggenheim C, Brand A, Buergmann H (2020) Niche partitioning of methane-oxidizing bacteria along the oxygen-methane counter gradient of stratified lakes. ISME J 14:274–287

Melton ED, Stief P, Behrens S, Kappler A, Schmidt C (2014) High spatial resolution of distribution and interconnections between Fe- and N-redox processes in profundal lake sediments. Environ Microbiol 16:3287–3303

Mendonça R, Barros N, Vidal LO, Pacheco F, Kosten S, Roland F (2012) Greenhouse gas emissions from hydroelectric reservoirs: what knowledge do we have and what is lacking? in: Liu GX (Ed.), Greenhouse Gases-Emission Measurement and Management Rijeka, InTech, pp. 55–77

Nie WB, Ding J, Xie GJ, Tian X, Lu Y, Peng L, Liu FB, XinG DF, Yuan ZG, Ren NQ (2021) Simultaneous nitrate and sulfate

dependent anaerobic oxidation of methane linking carbon, nitrogen and sulfur cycles. Water Res 194(5):116928
Norði KÁ, Thamdrup B (2014) Nitrate-dependent anaerobic methane oxidation in a freshwater sediment. Geochim Cosmochim Acta 132:141–150
Norði KA, Thamdrup B, Schubert CJ (2013) Anaerobic oxidation of methane in an iron-rich danish freshwater lake sediment. Limnol Oceanogr 58:546–554
Oni OE, Friedrich MW (2017) Metal oxide reduction linked to anaerobic methane oxidation. Trends Microbiol 25:88–90
Quadra GR, Sobek S, Paranaíba JR, Isidorova A, Roland F, do Vale R, Mendonça R (2020) High organic carbon burial but high potential for methane ebullition in the sediments of an amazonian hydroelectric reservoir. Biogeosciences 17:1495–1505
Riedinger N, Formolo MJ, Lyons TW, Henkel S, Beck A, Kasten S (2014) An inorganic geochemical argument for coupled anaerobic oxidation of methane and iron reduction in marine sediments. Geobiol 12:172–181
Rissanen AJ, Jilbert T, Simojoki A, Mangayil R, Aalto SL, Peura S, Jäntti H (2021a) Anaerobic oxidation of methane in sediments of a nitrate-rich, oligo-mesotrophic boreal lake. bioRxiv 426818
Rissanen AJ, Saarela T, Jäntti H, Buck M, Peura S, Aalto SL, Ojala A, Pumpanen J, Tiirola M, Elvert M, Nykänen H (2021b) Vertical stratification patterns of methanotrophs and their genetic controllers in water columns of oxygen-stratified boreal lakes. FEMS Microbiol Ecol 97:fiaa252
Rosentreter JA, Borges AV, Deemer B, Holgerson MA, Liu S, Song C, Melack JM, Raymond PA, Duarte CM, Allen GH, Olefeldt D, Poulter B, Batin TI, Eyre BD (2021) Half of global methane emissions come from highly variable aquatic ecosystem sources. Nat Geosci 14:225–230
Scholten JCM, Stams AJM (2000) Isolation and characterization of acetate-utilizing anaerobes from a freshwater sediment. Microb Ecol 40:292–299
Sela-Adler M, Ronen Z, Herut B, Antler G, Vigderovich H, Eckert W, Sivan O (2017) Co-existence of methanogenesis and sulfate reduction with common substrates in sulfate-rich estuarine sediments. Fronti Microbiol 8:766
Sivan O, Adler M, Pearson A, Gelman F, Bar-Or I, John SG, Eckert W (2011) Geochemical evidence for iron-mediated anaerobic oxidation of methane. Limnol Oceanogr 56:8
Su G, Niemann H, Steinle L, Zopfi J, Lehmann MF (2019) Evaluating radioisotope-based approaches to measure anaerobic methane oxidation rates in lacustrine sediments. Limnol Oceanogr Meth 17:429–438
Wassmann R, Neue HU, Bueno C, Lantin RS, Alberto MCR, Buendia LV, Bronson K, Papen H, Rennenberg H (1998) Methane production capacities of different rice soils derived from inherent and exogenous substrates. Plant Soil 203:227–237
Wells NS, Chen JJ, Maher DT, Huang P, Erler DV, Hipsey M, Eyre BD (2020) Changing sediment and surface water processes increase CH_4 emissions from human-impacted estuaries. Geochim Cosmochim Acta 280:130–147
Westermann P, Ahring BK, Mah RA (1989) Threshold acetate concentrations for acetate catabolism by aceticlastic methanogenic bacteria. Appl Environ Microbiol 55:514–515
Xiao KQ, Beulig F, Kjeldsen KU, Jorgensen BB, Risgaard-Petersen N (2017) Concurrent methane production and oxidation in surface sediment from Aarhus Bay, Denmark. Front Microbiol 8:1198
Yang H, Yu S, Lu H (2021) Iron-coupled anaerobic oxidation of methane in marine sediments: a review. J Mar Sci Eng 9:875

Authors and Affiliations

Xueping Chen[1] · Meilin Yang[1] · Jing Sun[1] · Juan Yu[1] · Lihua Liu[2] · Shuang Bai[1,3] · Fayan Bai[1] · Ming Yang[1] · Zheng Chen[4] · Chiquan He[1] · Xiaoyan Liu[1] · Jing Liang[5] · Fushun Wang[1]

Xueping Chen
xpchen@shu.edu.cn

Meilin Yang
mlyoung@shu.edu.cn

Jing Sun
jsunbk@connect.ust.hk

Juan Yu
yjenviro@shu.edu.cn

Shuang Bai
hoarfrost@shu.edu.cn

Fayan Bai
bfy0720@shu.edu.cn

Ming Yang
mingyang@shu.edu.cn

Zheng Chen
Zheng.Chen@xjtlu.edu.cn

Chiquan He
cqhe@shu.edu.cn

Xiaoyan Liu
lxy999@shu.edu.cn

Jing Liang
21643883@qq.com

[1] School of Environmental and Chemical Engineering, Shanghai University, 99 Shangda Road, Shanghai 200444, China

[2] Guangzhou Institute of Energy Conversion, Chinese Academy of Sciences, Guangzhou 510640, China

[3] Shanghai Kede Environmental Protection Testing Technology Consulting Service Co, Ltd, Shanghai 200235, China

[4] Department of Health and Environmental Sciences, Xi'an Jiaotong-Liverpool University, Suzhou 215123, Jiangsu, China

[5] Shanghai Academy of Landscape Architecture Science and Planning, Shanghai 200232, China